Nuclear Inst. and Methods in Physics Research, A 942 (2019) 162338

Contents lists available at ScienceDirect

Nuclear Inst. and Methods in Physics Research, A

journal homepage: www.elsevier.com/locate/nima

A novel synthetic diamond Cherenkov radiator for measuring space radiation

J.J. Connell [a,*], C. Lopate [a], J.W. Tabeling [b]

[a] Space Science Center, and Department of Physics and Astronomy, the University of New Hampshire, Durham, NH 03824, USA
[b] Applied Diamond, Inc., Wilmington, DE 19805, USA

ARTICLE INFO

Keywords:
Cosmic ray instruments
Solar energetic particle instruments
Cherenkov detectors
Spacecraft instruments
Diamond radiators

ABSTRACT

The measurement of cosmic rays and Solar energetic particles in space is basic to our understanding of the Galaxy, the Sun, phenomena in the Heliosphere and the emerging field of space weather. For these reasons, cosmic ray instruments are common on both scientific spacecraft and operational spacecraft such as weather satellites.

Cosmic rays (CRs) and Solar energetic particles (SEPs) include ions over the full range of elements found in the Solar System. High-resolution measurements of the energy spectra of space radiation are key to understanding both acceleration and propagation processes. An inherent challenge is the large range of energies of such spectra. Cosmic ray energies range up to over 10^{21} eV, while SEPs can reach a few GeV. Multi-instrument measurements are currently required to cover the full range of particle energies. Indeed, the highest energy particles, due to the rarity, can only be measured with ground-based instruments using the atmosphere as a calorimeter.

Over limited energy ranges, SEP spectra are often approximated by a power law; however, over the full energy range, SEP events exhibit changing spectral shapes (e.g. "knees", "roll-overs" and "cut-offs"). These features give information about the acceleration processes, such as size of the acceleration region, time of acceleration, morphology of the magnetic field during acceleration, and others, all of which can vary from event to event. Measurements of such features are often compromised by the need to combine measurements from more than one instrument, each with its own limited energy range. Even if there are no gaps between the energy intervals of the instruments, differing systematics can severely impact data analysis. A single instrument capable of measurements over a continuous and extended energy range would offer vastly more reliable measurement of the energy spectra of SEP events as well as replacing multiple instruments on resource-limited spacecraft.

The most common method to measure GCRs and SEPs from a few to ~100 MeV for protons, is Si Solid-State Detector (SSD) stacks. Above these energies, Cherenkov detectors are typically used together with SSDs. Ideally, to provide full energy coverage with no gaps, this requires a Cherenkov radiator with a threshold of ~100 MeV. No suitable Cherenkov detector with such a low threshold has been developed. We are in the process of developing a synthetic diamond Cherenkov detector for this purpose. Diamond's high index of refraction (2.42) results in a theoretical threshold of 92 MeV for protons. Even with a practical threshold of ~110 MeV, this is ideal for extending the energy range from that of SSDs alone to that of sapphire Cherenkov detectors (202 MeV threshold) with higher energies attainable using plastic Cherenkov detectors. Both Sapphire and plastic Cherenkov radiators have spaceflight heritage.

1. Introduction

Energetic charged particle studies permeate and thread much of the science of the Heliosphere, including studies of acceleration in Solar particle events, understanding the propagation of shocks in both the inner and outer Heliosphere, and studies of the transport of those particles and other energetic particles throughout the Heliosphere, to name a few. Energetic particles are both a subject of study in their own right, and a tool to study other phenomena such as flares, shocks, magnetic reconnection, flux tubes, etc. The effects of energetic particles in the relevant energy range (10's to 100's of MeV/u) on man-made systems in space has long been recognized and includes total ionizing dose as well as single events effects (SEE) such as single event upsets (SEU), single event latchups (SEL) and single event burnout (SEB) [1]. These radiations also impact humans in space. Beyond the Earth's magnetosphere, the largest Solar Particle Events (SPEs) have the potential to cause acute radiation syndrome in astronauts [2], while less extreme

* Corresponding author.
E-mail address: james.connell@unh.edu (J.J. Connell).

https://doi.org/10.1016/j.nima.2019.162338
Received 3 June 2019; Received in revised form 28 June 2019; Accepted 1 July 2019
Available online 3 July 2019
0168-9002/

exposure increase the risk of cancer. It is impractical to shield space system from 200 MeV protons, or ions with comparable penetration.

Understanding charged particle acceleration in the Heliosphere aids in understanding astrophysics. The late John A. Simpson often remarked that "The Heliosphere is a laboratory for astrophysics" [3]. For example, stochastic or Fermi acceleration of charged particle by shocks in plasmas occurs on all scales in space, from planetary magnetospheres, to Coronal Mass Ejections (CMEs) to Corotating Interaction Regions (CIRs) to the termination shock to supernovae shocks to shocks from astrophysical jets from compact stellar objects, to shocks in the intergalactic medium from jets from active galactic nuclei. The one major difference between these astrophysical and Heliospheric phenomena, aside from scale, being that in-situ measurements are possible, for the foreseeable future, only in the Heliosphere.

For all these reasons, energetic charged particle instruments are found on many space science missions and as space weather instruments on operational satellites. Particle energies in SPEs often extend up to a few hundred MeV for protons (and in some instances, over 1 GeV). The energy spectra of these energetic particles often include key features at higher energies. Spectra often show "roll-overs", "knees" or "cut-offs" at higher energies. Different acceleration (energy pumping, e.g. Schwadron & McComas [4], versus stochastic versus first-order Fermi, e.g. Webb [5]) or transport theories (drift dominated, e.g. Pesses, et al. [6] versus random walk of field lines, e.g. Jokipii, [7] versus global Solar magnetic field rotation, e.g. Fisk, [8]) predict different behavior of energetic charged particles as a function of energy. When multiple instruments are used to try to continuously cover the energy range of energetic particles up to hundreds of MeV, there are natural concerns about changes in the measured energy spectra being instrumental artifacts rather than real differences in the particle spectra.

An example of the value of a single instrument capable of producing accurate differential energy charged particle measurements continuously over the full energy range from ~10 MeV to ~1 GeV can be seen in Figure 4 in Lovell et al. [9]. The plot shows spectra from 1 MeV to 10 GeV for the 29 September 1989 SEP event. Space instrument data extends only to ~200 MeV. Beyond that, spectra are inferred using ground-based neutron monitor data. The change in the spectral shape, occurring between 300 and 1000 MeV, is fit with a model that includes an exponential rollover. However, the lack of continuous differential energy measurements makes such a fit somewhat problematic. It would be impossible, for example, to differentiate between such an exponential rollover and a double power-law spectrum — and the difference between these models has consequences on the true acceleration process for these particles and their transport in space. It is problematic that the change in spectral shape occurs from 300 to 1000 MeV — as that is the energy region where data is largely unavailable. Continuous space-based measurements from 10 MeV to 1 GeV, *ideally from a single instrument*, would be invaluable in determining the actual shape of the spectra for large SPEs, especially since such spectral changes can take place at almost any energy. For many Solar particle events, having continuous energy measurements up to just 250 MeV would reveal spectral features. An instrument using diamond, sapphire and plastic Cherenkov scintillators could be used not only for Solar and Heliospheric studies, but also for Galactic cosmic ray studies, as it would extend over the peak of the GCR proton spectrum at ~500 MeV.

As they have the highest velocities, energetic ions accelerated to 100s of MeV/u, and electrons accelerated to 10s of MeV, will be the first particles arriving at Earth from Solar particle events. The unambiguous detection of these particles would aid in Space Weather forecasting (e.g. Posner [10]) — especially as the detection of these particles would indicate a good magnetic connection between the accelerating site and the Earth, thus heralding the flood of much higher fluence but less energetic particles to follow. Accurate and precise measurements of these would allow the differentiation of energetic model predictions (for example between focused transport and diffusive transport).

Thus, a single energetic charged particle instrument able to measure protons (and He ions) over a continuous energy range from ~10 MeV (MeV/u) to ~700 MeV (MeV/u) in space with good ($\leq$ 20%) energy resolution would thus be extremely valuable to the study of space radiation. Heavy ions could also be measured with similar velocity/penetrations.

2. Instruments using Si solid-state detectors (SSDs)

For energies of ~1–100 MeV for protons (and energies with corresponding penetration for heavier ions) the Si solid-state detector is the primary basis for space-based instruments. These detectors are robust (especially in the vacuum of space, where surface contamination is not an issue) and provide high precision measurements. Signals, to high order, are proportional to particle energy depositions. Instruments typically employ a stack of SSDs, each measuring energy loss (dE/dx). For particles that stop in the stack, the total energy can be determined by summing the signals. By looking at the energy loss at, or near, the top of the stack (dE/dx) versus the residual energy (E'), particle species and energy can be determined.

For particles that penetrate the stack, another technique is required. This uses the change in energy loss rate as an energetic charged particle penetrates the instrument stack. This is termed the multiple dE/dx technique. At the initial (highest) particle energy, the energy loss will be relatively low. Thus an SSD at, or near, the top of the instrument will produce a relatively small signal. As the particle traverses the stack, it losses energy, so that the signal from a detector at, or near, the bottom of the stack will be larger. As the incident particle energies increase, the energy loss through the stack decreases. Thus, the difference in signal between the detectors becomes progressively smaller and the incident energy of the particle will be estimated with decreasing precision. Eventually, measurement uncertainties become too large to determine a useful incident energy.

A simple example would be a telescope consisting of four 1500 um thick Si solid state detectors (D1-4). For particles stopping in D2-4, high resolution measurements as to species and total energy are easily obtained using the energy loss (dE/dx) versus residual energy (E') technique (e.g. Connell et al. [11] and references therein). For particles that penetrate D4, the multiple dE/dx method is required. Fig. 1 shows the difference between energy losses measured in D4 and D1 (blue points) vs. energy at the top of the telescope for protons. As the proton passes through D1-4, it is slowed by energy loss and the signal increases with decreasing velocity. So long as the change in energy loss is detectable, the particle incident energy can be estimated. The red points are the same data with 35 keV of random detector noise (the dominant source for protons) included. Energy resolution is lost with increasing energy. The mean value is 1-σ from zero at ~110 MeV, marking the upper limit of energy discrimination using SSDs alone. Extending the energy reach of the SSD stack alone to 200 MeV would require about eight additional 1500 um SSDs. This is often impractical and never desirable as power and mass increase while the geometrical factor decreases with increasing numbers of SSDs.

One complication should be noted: space radiation is isotropic, or nearly so. Thus particles enter an instrument at all angles, and corrections for their pathlengths through active detectors are required for high precision heavy ion identification. This can be accomplished using hodoscopes or other techniques such as the Angle Detecting Inclined Seniors (ADIS) [12].

To extend the energy reach of pure SSD based instruments, Cherenkov detectors are typically added to the instrument stack.

Unfortunately, no Cherenkov radiator has yet been flown in space instruments with a threshold so low as 100 MeV. Thus, a gap exists between energies easily measured with SSDs, and energies accessible with Cherenkov detectors. We propose an innovative synthetic diamond Cherenkov radiator, and have recently been funding to develop such a detector (NASA grant 80NSSC18K1253).

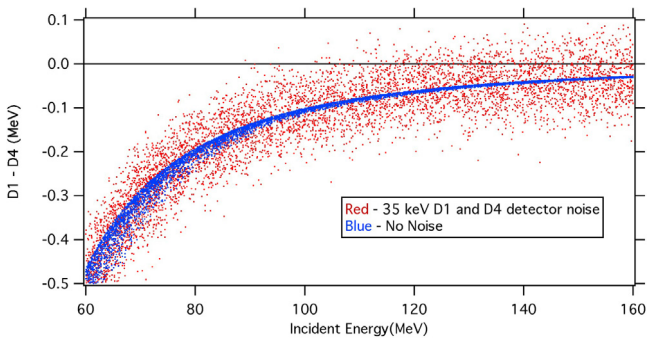

Fig. 1. Monte Carlo modeled telescope response for particles penetrating D4 using the multiple dE/dx technique. D1 minus D4 energy losses vs. energy at the top of the telescope for protons are shown. Out of geometry particles are suppressed by excluding events that trigger a surrounding anti-coincidence scintillator shield (S) similar to that in Fig. 5. The blue points show the results without detector noise, while the red points include 35 keV detector noise. The scatter in the blue points arises from the different angles of incidence of the protons. When the difference between the D1 and D4 energies becomes, with 1-σ uncertainty, indistinguishable from 0, this method of determining the incident particle energy becomes unreliable. For this simple detector scheme, when proton energies exceed ~110 MeV a reliable energy determination using the dE/dx technique is not possible.

3. Cherenkov light and detectors

Cherenkov light is emitted when a charged particle traverses a medium at a velocity greater than the speed of light in the medium, $c_n = c/n(\omega)$ [13]. The classic analogy is the sonic boom of a supersonic aircraft. The only requirement for Cherenkov emission is that the medium be transparent at the given frequency, and that the charged particle be moving above the speed of light for that frequency. The light is emitted in a forward cone with characteristic Cherenkov angle. Particle detectors using Cherenkov light can be broadly classed into two types: Imaging Cherenkov detectors that measure the cone angle (e.g. Ring Imaging CHerenkov, RICH [14]); and light integrating Cherenkov detectors which measure the total light output from a radiator. We focus on the simpler light integrating Cherenkov detectors.

For Cherenkov detectors working in the optical and near optical (the vast majority), dispersion is typically sufficiently small that the index of refraction, n, is treated as constant. Provided the medium is transparent over the detection range of a typical photomultiplier tube (PMT) ~350–550 nm, the integrated light output is [14]

$$dN/dy = \sim 500\ z^2 \sin^2\theta_C\ (\text{photons/cm}) = \sim 500\ z^2(1-1/\beta^2 n^2)\ (\text{photons/cm}) \quad (1)$$

Here $\beta = v/c$, z is the charge number (in e) of the incident particle and y is the distance in cm (as opposed to areal density which we shall denote by x) traversed in the medium.

A number of points arise from the above: (1) The transparency and index of refraction are effectively the sole determinant of Cherenkov light emission. Material properties, such as density, have no direct role. (2) The index of refraction, n, determines the minimal velocity and hence the minimal energy (Cherenkov threshold) for a given species that will produce Cherenkov light; and a higher n corresponds to lower energy thresholds. (3) Total light output is modest. The Poisson statistics relating to light collection efficiency and the light detection system are usually the dominant factor in resolution. (4) As the particle energy increases, $\beta \to 1$, and the Cherenkov light approaches a saturation level. The saturation level depends upon n, with a higher index providing a higher saturation light output.

The functional form of the Cherenkov emission dN/dy is very different from the ionization energy loss dE/dx, which is the reason telescope designs often combine Cherenkov detectors with ionization energy loss detectors (SSDs, scintillators, etc.). In space radiation telescopes, Cherenkov detectors have mainly been used to (1) to extend the energy reach of a telescope for penetrating particles (usually ions) and (2) to distinguish (the often rarer) electrons of a given energy from (the often more abundant) protons. Ideally, and often in practice, the latter is accomplished by the protons being below Cherenkov threshold, while the electrons of the same energy (but lower mass) have ~43 times the velocity, thus producing a Cherenkov signal near saturation, giving a particularly clean measurement.

A major advantage of Cherenkov detectors is the ability to tune an instrument's response to attain a specific energy range by choosing a material with suitable n. Conversely, the challenge is often finding a suitable radiator material with the desired n (see Table 1). Liquid radiators, with water being common, and gas radiators are also widely used. Finally, aerogels have been used, giving intermediate indices of refraction and avoiding the practical difficulties (particularly in space) of liquids and gases. Telescopes may use more than one Cherenkov detector with different radiators having a progression of indices of refraction (e.g. the Kiel Electron Telescope (KET) on *Ulysses* [15]).

Fig. 2 shows the calculated light output for protons normally incident on a 1.6 cm Cherenkov detector using diamond (black trace) and neglecting energy loss (thus, idealized). Also shown is the light output taking energy loss into account, for diamond (red), sapphire (blue) and Lucite (green). Note that some plastics for Cherenkov detectors are doped with waveshifters (e.g., Pilot-425) to increase the light output over Lucite alone (which is shown). The lower threshold energy, and higher light output for diamond compared to sapphire is readily apparent.

While particles do lose energy through Cherenkov emission, it is negligible compared to ionization energy loss. When modeling Cherenkov emissions from a radiator of finite thickness, it is necessary to calculate the energy loss (dE/dx), taking into account the changing velocity of the particle, which may fall below Cherenkov threshold, as the particle traverses the radiator. The effect is also apparent in Fig. 2. Compared to the trace without dE/dx (black), the trace with energy loss for diamond (red) has a more gradual onset owing to the proton dropping below threshold part way though the radiator. The traces converge at higher energy as the proton remains at, or near, saturation energy throughout its path in the radiator.

A diamond Cherenkov detector would extend the energy reach of a single energetic charged particle telescope from the ~100 MeV for standard SSD-based instruments to ~250 MeV, more than doubling the energy reach, while lowering the mass and power necessary to achieve the same counting statistics.

4. Synthetic diamond as a Cherenkov radiator

A challenge has been finding materials with higher n to extend the energy reach to lower energies. So far as the authors know, the highest n material used in a space telescope is lead-fluoride ($n = 1.89$) in KET on *Ulysses* [15]. Sapphire ($n = 1.77$), e.g. in the Cosmic Ray Nuclear Composition (CRNC) instrument on IMP-8 [16,17] has been more widely used. While sapphire has issues with residual scintillation (see below), its lower density is an advantage over lead-fluoride for space missions. (The KET, in part, used lead-fluoride as a calorimeter where its high density was advantageous.) We concentrate on sapphire, recognizing that lead-fluoride's Cherenkov response is very similar (Table 1).

The availability of synthetic diamond offers a new Cherenkov radiator material with a much higher index of refraction ($n = 2.42$), providing a lower energy threshold (Table 1) and higher light output for a given radiator thickness (Fig. 2).

Synthetic diamond (see Fig. 3) can now be manufactured in relatively large (~2.5 in. diameter) wafers of significant thickness (~0.5 mm) making stacks of the material suitable for space-based charged particle telescopes. Applied Diamond is a leader in producing such very high purity Chemical Vapor Deposited (CVD) diamond

Table 1
Cherenkov radiators characteristics.

	Synthetic diamond	Lead-fluoride	Synthetic sapphire	Pilot-425(Lucite)
Index of refraction	2.42	1.89	1.77	1.51
Density	3.52 g/cm^3	~7.7 g/cm^3	3.97 g/cm^3	1.18 g/cm^3
Proton threshold	92 MeV	167 MeV	202 MeV	310 MeV
Electron threshold	51 keV	91 keV	110 keV	175 keV
Residual scintillation	<3%		~20%	~5%

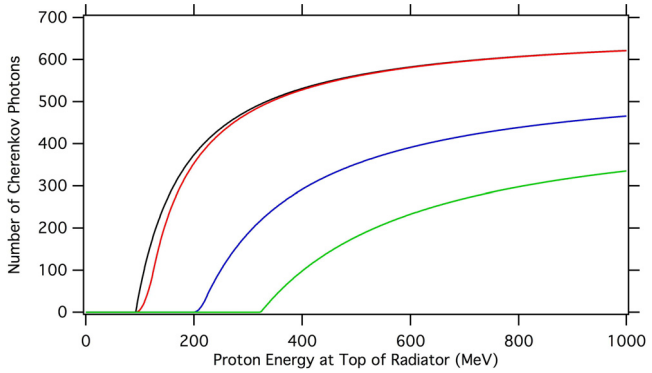

Fig. 2. Calculated Cherenkov light emission in 1.6 cm radiators from normal incidence energetic protons. Black curve is for synthetic diamond neglecting proton energy loss; red is the same, but including energy loss; blue is for sapphire including energy loss; green is for Lucite including energy loss. Residual scintillation is not included.

Fig. 3. Chemical Vapor Deposited (CVD) synthetic diamond sample produced by Applied Diamond, Inc. The clarity of the card seen through the sample strikingly demonstrates the suitability of the material for a Cherenkov radiator. (Picture courtesy Applied Diamond, Inc.).

wafers. The diamond wafer is transparent significantly beyond the response range of a PMT, making it well suited for Cherenkov radiators. The amorphous structure results in only very slight light scattering that would have little impact on a Cherenkov detector. (Aerogel radiators have far worse scattering properties, yet are widely used.) Similarly, scattering at the interfaces between this stacked layers of diamond should mainly result in addition light diffusion.

We know of only one previous use of synthetic diamond as a Cherenkov radiator for energetic charged particles [18]. The goal was to measure runaway electron pulses from instabilities in a tokomak plasma. A Cherenkov detector was chosen to isolate the energetic electrons in an environment filled with bremsstrahlung and thermal X-rays. A high index of refraction for the Cherenkov was required because of the energy of the electrons. Rutile (TiO_2) crystal (n = 2.90) was considered. but rejected because of relatively poor thermal conductivity. Rutile is unsuited to most Cherenkov applications owing to its poor transparency – it is visibly reddish-brown – but could be used in small radiators, as was all that was required in this application. The synthetic diamond probe proved successful.

Cherenkov light from a relativistic electron beam in a single crystal diamond has been studied [19] on a more fundamental basis to understand such effects as particle channeling.

5. Energy resolution

The energy resolution of a light-integrating Cherenkov detector can be estimated using the shape of the energy response curve (Fig. 2) and the photoelectron statistics,

$$\sigma_E \approx (dP/dE)^{-1} * sqrt(P) \quad (2)$$

where P is the number of photoelectrons, related to N by the light collection efficiency and quantum efficiency of the electronic detector. Using a 1.6 cm radiator and assuming a light collection efficiency of 70% (reasonable for a small light diffusion box), a quantum efficiency of 30% (typical of a PMT), and including ionization energy loss in the radiators, gives the energy resolution shown in Fig. 4 for synthetic diamond (red), sapphire (blue) and Lucite (green). Energy resolution near threshold reflects the steep increase in light emission with energy. At the lowest energy, the resolution is more theoretical than practical: a practical threshold of 10 photoelectrons (p. e.) corresponds to 115 MeV with the diamond radiator, 228 MeV with sapphire and 337 with Lucite.

The jog at the bottom of the diamond and, to a lesser degree, the sapphire curves, results from the shape of the response curves convoluted with the p. e. statistics. The relevant response curves (Fig. 2) show a complicated, concave-like curvature at low energy (most noticeable for diamond) due to the energy loss process and the depth at which the proton falls below Cherenkov threshold in the radiator. The jogs are the result. As the energy loss plays a greater role at low energy, the jog is most noticeable in the diamond curve, less in the sapphire, and not at all for the plastic, in line with their energy thresholds. The slightly jagged details in the jogs are an artifact of the finite modeling.

As shown in Fig. 4, a diamond Cherenkov would provide good differential energy resolution (< 15%) for protons from about 115–200 MeV, with adequate (20%), resolution up to 250 MeV (as shown as a dashed line in Fig. 4). An integral flux for protons above ~300 MeV would also be possible. This capability alone would be extremely useful for studying Solar Energetic Particles. The plot also shows that a diamond Cherenkov could be used in conjunction with a sapphire Cherenkov and with a Lucite radiator, with each picking up where the former loses resolution. A telescope using solid-state detectors, a diamond Cherenkov, a sapphire Cherenkov and a Lucite Cherenkov could provide continuous energy coverage, at a 20% or better statistical sampling, from a few MeV to ~ > 700 MeV.

6. Directionality

While as noted, the main roles of Cherenkov detectors in space radiation telescopes has been to extend the energy reach and distinguish electrons from protons, a secondary role has often been distinguishing upwards from downwards moving particles, particularly in integral flux measurements (e.g., CRNC on IMP-8 [16,17]). As Fig. 1 clearly shows, for instruments using SSDs alone, at higher energies it becomes impossible to distinguish upward and downward passing particles. If the instrument has clear viewing cones both forward and back, it can simply operate in a bidirectional mode. In most cases, the rear of the

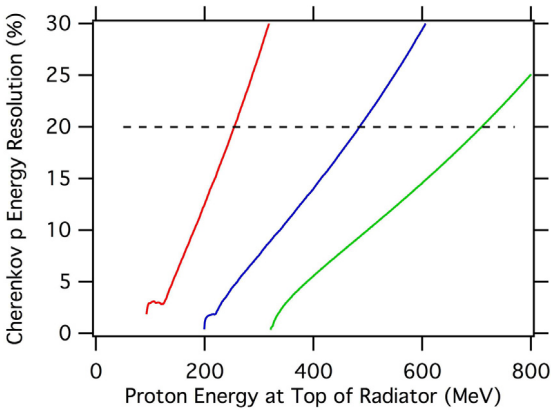

Fig. 4. Calculated Cherenkov proton fractional energy resolution (1-σ) for 1.6 cm radiators with 70% light collection efficiency and 30% PMT quantum efficiency. Proton energy loss (dE/dx) is included. Red trace is for synthetic diamond; blue is for sapphire; green is for Lucite. The horizontal black dashed line shows the energies above which the resolution of each Cherenkov radiator becomes worse than 20%.

instrument is obstructed by the spacecraft and integral fluxes must be corrected by subtraction with – often major – systematic errors.

Detectors that measure the Cherenkov light cone are inherently direction sensitive as the light cone is in the direction of the particle velocity. Directional sensitivity in light integrating Cherenkov detectors then arises from asymmetries in the design of the detector's light collection or conversion system. For example, Cherenkov radiators are often coated with waveshifting paint on the bottom (and perhaps the sides) but not the top. This arrangement will produce less light for upwards passing particles than downward passing [20].

7. Residual scintillation in Cherenkov detectors

A significant concern for Cherenkov radiators used in light integrating mode is residual scintillation. (Imaging Cherenkov detectors are less affected as scintillation is isotropic.) Plastic Cherenkov radiators typically have residual scintillation levels of ~5%. Sapphire radiators may have much higher residual scintillation: the sapphire radiator used on CRNC for IMP-8 had a residual scintillation of 28% [21]. It is known [22] that natural diamond scintillates (in the radiation detector sense) and from a patent [23] that some synthetic diamond does as well. In the latter case, however, the disclosure emphasized enhancing scintillation with doping, indicating that the type and levels of impurities were crucial in diamond scintillation. The CVD diamond manufactured by Applied Diamond has particularly low and controllable impurity levels.

The one known use of synthetic diamond as a Cherenkov radiator [18] exposed the diamond to very extreme levels of both thermal and bremsstrahlung X-rays. Thus, any scintillation would have been extreme — despite which the measurement was successful. However, the experiment also used relatively high-speed electronics, which would have suppressed scintillation so this application provided no definitive insight on the issue. We plan to measure residual scintillation in synthetic diamond with varying levels of nitrogen impurities.

Even if the level of residual scintillation in the pristine diamond is acceptable, in a space application, radiators will be exposed to ionizing radiation that could increase both scintillation and light absorption in the diamond. A major impetus for the development of diamond-based solid state detectors is radiation hardness up to at least 10 Mrads [24], suggesting that Total Ionizing Doses (TIDs) up to these levels are unlikely to be a concern. However, it is also known that gem diamonds are exposed to radiation (together with heat treatments) to introduce color for esthetics. The TIDs are 100s to 1000s of Mrads [25], but the results are visible to the naked eye. On the positive side, the faint coloring indicates, simply by eye, that transparency is only slightly impaired even at these extreme doses. Scintillation in irradiated diamond is potentially a concern. We plan to expose a number of samples from Applied Diamond to proton radiation from ~100 krad to at least 10 Mrad. Protons (as opposed to γ- or β-rays) will be used since they produce defects from ionization, crystal displacement and nuclear spallation. The samples will be characterized for transparency and scintillation pre- and post-irradiation.

8. Modeling of a telescope with a diamond Cherenkov detector

To appreciate the impact of a diamond Cherenkov detector, it is best viewed in the context of an instrument. Fig. 5 shows a simple concept of our telescope design. The telescope is cylindrically symmetric. The entrance aperture begins with four 1500 μm thick Si solid-state detectors (D1-4). Below these are the three Cherenkov detectors, with 1.6 cm cylindrical diamond (C1), sapphire (C2) and Lucite (C3) radiators. Between the Cherenkov detectors are 1500 μm thick Si SSDs (D5-7). Penetrating particles are identified by the Si SSD at the bottom (R). A trajectory system at the top of the instrument stack, such as position sensing detectors or ADIS [11,12,26] could be included in a future telescope for heavy ion composition measurements. We plan detailed modeling of a similar instrument.

For the purposes of this paper, a truncated version (D1-5 and the diamond Cherenkov, C1) has been modeled using Monte Carlo simulations. For particles stopping in D2-4, high resolution measurements as to species and total energy are easily obtained using the energy loss (dE/dx) versus residual energy (E') technique with Si SSDs alone (e.g. Connell et al. [12] and references therein). For particles that penetrate D4, the multiple dE/dx method is required, as discussed in Section 2 and seen in Fig. 1. The mean value of the measurement is 1-σ from zero at ~110 MeV, marking the upper limit of energy discrimination using SSDs alone.

Fig. 6 (left panel) shows the calculated light output from the nominal 1.6 mm diamond Cherenkov detector vs. energy at the top of the telescope. (Onset is at higher energy compared to Fig. 2 because the energy shown is at the top of the telescope, not top of the radiator as in Fig. 2.) The spreading of signal at higher energies arises from particles passing through the radiator at off-normal angles resulting in increased pathlength. At low energies, this is absent as the proton's energy falls below threshold while inside the radiator, making the effective pathlength angle independent. Fig. 6 (right panel) shows the photoelectrons for the same data with a 70% light collection efficiency and 30% quantum efficiency and including statistical fluctuations. As seen in Fig. 2, energy resolution in this model remains good up to 200 MeV (≤15% statistical uncertainty) and useful up to ~250 MeV (≤20% statistical uncertainty).

While the above has concentrated on proton measurements. ^{4}He would provide almost identical results since the energy loss goes as $\sim Z^2/A$ ~1. Resolution in the SSD detectors would be improved because of the larger signals compared to detector noise. Performance of the diamond Cherenkov detectors would be improved with the increase in light output — four times the number of photons providing approximately twice the resolution.

9. Impact on resource requirements

Any instrument for space flight faces constraints on mass, power and telemetry. For charged particle telescopes, the mass is most often the design driver, with power a close second, and telemetry a distant third.

A simple (no margin or contingency) mass estimate for a realistic space telescope alone (no electronics) for the design concept similar to Fig. 5, but with only the diamond Cherenkov, including radiator and PMTs, is 200 g. This assumes a 300 mm^2 active area for the detectors. For comparison, to achieve an energy limit of 200 MeV for protons (still below the 250 MeV performance of the telescope with Cherenkov

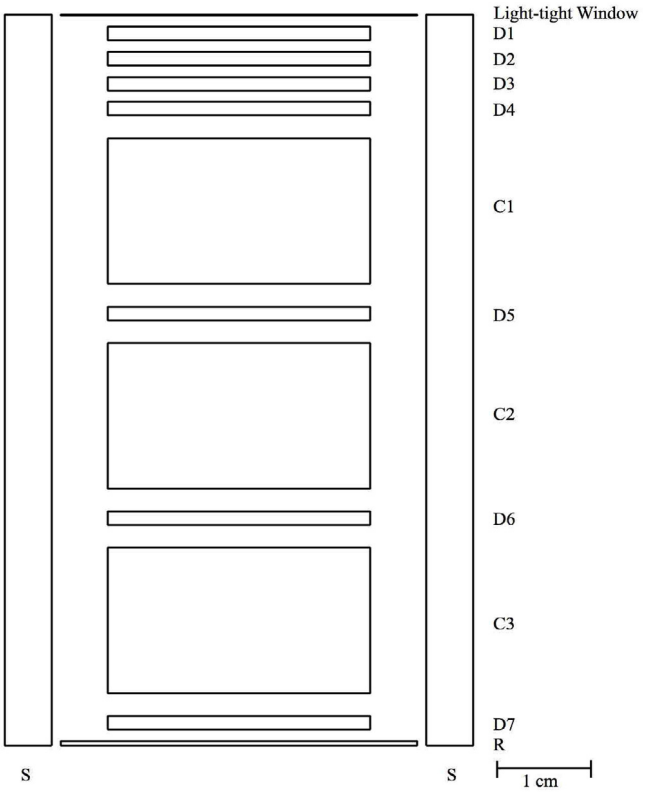

Fig. 5. The concept telescope, cylindrically symmetric with an entrance of 4 Si solid state detectors (D1-4), and three Cherenkov detectors, diamond (C1), sapphire (C2) and Lucite (C3) with Si SSDs (D5-7) between. Penetrating particles are identified by a Si SSD at the bottom (R). A surrounding plastic scintillator cylinder detects out of geometry events. Total length is approximately 7.5 cm.

detector) requires the addition of eight Si SSDs as noted in Section 2. Mounting additional SSDs effectively doubles the instrument length. The geometrical factor decreases with length squared, so to attain the same collection power and similar performance, the SSD-only design requires 1200 mm^2 detectors resulting in a mass of 300 g, ~50% higher. The SSD-only telescope, with the numbers of detectors increased to reach 250 MeV, would be still heavier.

The impact of the telescope designs on electronics needs also to be considered. The diamond Cherenkov adds but a single analog channel to the electronics, while eight additional SSDs, even ganged, would add more. The impact on power and mass would depend very much upon the actual design. A conventional design with large dynamic range for heavy ions and active baseline restore (such as we use in GOES/EHIS) would add ~100 g and ~200 mW per channel. An ASIC-based design might add very little mass if channels on the chip are otherwise unused, so ~25 mW per channel. A PMT will require high voltage bias at ~1000 VDC, but thick (1500um) Si SSDs require biasing at ~250 VDC. The delta in taking the bias supply up to 1000 VDC, with the detector bias taken off at an intermediate stage adds less than 10% to the mass of the bias board.

Thus, a diamond Cherenkov detector would offer a major improvement over purely SSD-based energetic charged particle telescopes by extending their energy range with continuous coverage up to ~250 MeV (with integral fluxes above). Furthermore, the Cherenkov would provide unambiguous electron identification down to ~60 keV (top of the radiator).

Extending an SSD only telescope to 700 MeV would not be feasible. A sapphire Cherenkov would further extend the energy up to the point where a plastic Cherenkov detector would be effective. Incorporating both a sapphire and plastic Cherenkov detector with the same instrument cross section (300 mm^2) would result in a mass of estimate of 430 g. Expanding to 1200 mm^2 to compensate for the increased length would result in a mass of 740 g.

10. Conclusions

It is extremely rare for a new Cherenkov radiator material to become available for space instruments. So far as we know, the most recent were aerogel used on HEAO C3 (launched 1979) [27] and lead-fluoride used for the Kiel Electron Telescope (KET) on *Ulysses* (launched 1990, but developed long before) [15]. Synthetic diamond wafers now available, used as Cherenkov radiators, would significantly lower the available energy threshold.

A diamond Cherenkov detector, in concert with Si solid-state detectors, provides a scheme for a high energy particle telescope with significant advantages in mass, power and energy reach to a SSD only telescope. The addition of sapphire and plastic Cherenkov detectors offers the possibility of an instrument making proton measurements from a few MeV to ~700 MeV and He from a few MeV/u to ~700 MeV/u. This would be unprecedented in a single space-based instrument. Data from such an instrument would provide energy spectral shapes without the systematics currently inherent in combining data from two or more instruments as is currently required.

Under the recently awarded NASA grant 80NSSC18K1253, we will be further developing the diamond Cherenkov concept. This included additional Monte Carlo modeling; testing of diamond samples with

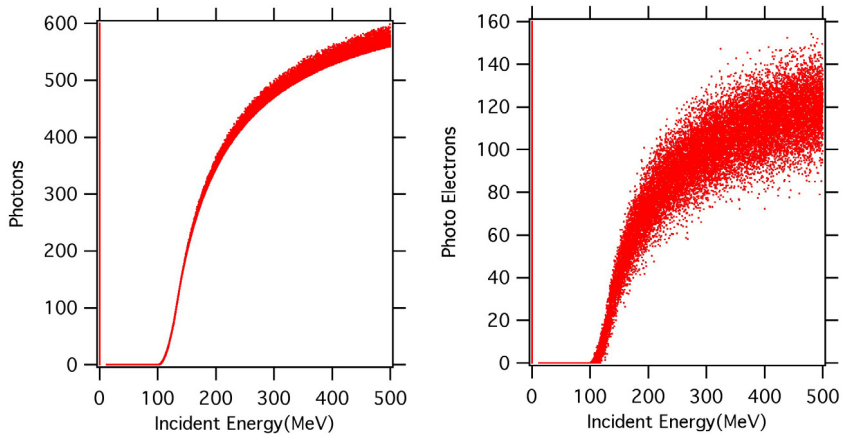

Fig. 6. Modeled telescope Cherenkov light signal for protons penetrating D4 in the notional telescope. Events that trigger S (the side) are excluded. Shown left is the expected number of photons. Broadening is due solely to variations in pathlengths due to various angles of incidence. Protons at lower energies drop below threshold in the radiator and show no pathlength effect. Shown right are the number of photo-electrons (p.e.) including Poison fluctuations.

varying levels of contaminants for residual scintillation; testing optical properties and residual scintillation of samples before and after irradiation by protons; building a test model telescope similar to Fig. 5 and exposing it to protons at an accelerator and to atmospheric muons.

While this paper has focused on charged particle instruments for space application, a practical diamond Cherenkov detector likely would also have other application in fields requiring radiation measurements. Such other possible applications are of particular interest to Applied Diamond, Inc.

Acknowledgment

This research was supported by the University of New Hampshire, USA.

References

[1] D.L. Chenette, J. Chen, E. Clayton, T.G. Guzik, J.P. Wefel, M. Garcia-Munoz, C. Lopate, K.R. Pyle, K.P. Ray, E.G. Mullen, D.A. Hardy, The CRRES/SPACERAD heavy ion model of the environment (CHIME) for cosmic ray and solar particle effects on electronic and biological systems in space, IEEE Trans. Nucl. Sci. 41 (1994) 2332–2339.

[2] J.L. Parsons, L.W. Townsend, Interplanetary crew exposure estimates for the 1972 solar particle event, Radiat. Res. 153 (2000) 729–733.

[3] J.J. Connell, private communication.

[4] N.A. Schwadron, D.J. McComas, The dynamic 3D heliosphere: Implications for and new sources of its energetic particles, Adv. Space Res. 32 (4) (2003) 531–543.

[5] G.M. Webb, First order and second order Fermi acceleration of energetic charged particles by shock waves, Agron. J. 270 (1983) 319–338.

[6] M.E. Pesses, J.R. Jokipii, D. Eichler, Cosmic ray drift, shock wave acceleration, and the anomalous component of cosmic rays, Astrophys. J. Lett. 246 (1981) L85.

[7] J.R. Jokipii, Cosmic ray propagation. I. Charged particles in a random magnetic field, Agron. J. 146 (1966) 480–487.

[8] L.A. Fisk, Motion of the footpoints of heliospheric magnetic field lines at the Sun: Implications for recurrent energetic particle events at high heliographic latitudes, J. Geophys. Res. 101 (A7) (1996) 15547–15553.

[9] J.L. Lovell, M.L. Duldig, J.E. Humble, An extended analysis of the 1989 cosmic ray ground level enhancement, J. Geophys. Res. 103 (A10) (1998) 23733–23742.

[10] A. Posner, Up to 1-hour forecasting of radiation hazards from solar energetic ion events with relativistic electrons, Space Weather 5 (2007) S05001.

[11] J.J. Connell, C. Lopate, R.B. McKibben, The angle detecting inclined sensors (ADIS) system: Measuring particle angles of incidence without position sensing detectors, Nucl. Instrum. Methods Phys. Res. A 457 (2001) 220–229.

[12] J.J. Connell, C. Lopate, K.R. McLaughlin, Accelerator test of an improved angle detecting inclined sensor (ADIS) prototype with beams of ^{78}Kr and fragments, Nucl. Instrum. Methods Phys. Res. A 837 (2016) 11–15.

[13] William R. Leo, Techniques for Nuclear and Particle Physics Experiments: A how-To Approach, second ed., Springer-Verlag, New York Berline Heidelberg, 1994.

[14] K.H. Althoff, Twenty-five years experience with cherenkov detectors in bonn, Nucl. Instrum. Methods Phys. Res. A 248 (1986) 39–52.

[15] J.A. Simpson, J.D. Anglin, A. Balogh, M. Bercovitch, J.M. Bouman, E.E. Budzinski, J.R. Burrows, R. Carvell, J.J. Connell, R. Ducros, P. Ferrando, J. Firth, M. Garcia-Munoz, J. Henrion, R.J. Hynds, B. Iwers, R. Jacquet, H. Kunow, G. Lentz, R.G. Marsden, R.B. McKibben, R. Mueller-Mellin, D.E. Page, M. Perkins, A. Raviart, T.R. Sanderson, H. Sierks, L. Treguer, A.J. Tuzzolino, K.-P. Wenzel, G. Wibberenz, The ulysses cosmic ray and solar particle investigation, Astron. Astrophys. Suppl. Ser. 92 (1992) 365–399.

[16] G.M. Mason, W.W. Mixon, University of Chicago charged particle experiments on *IMP7* and *IMP8*: Instrument and data format descriptions, NSSDC, Experiment ID 73-078a-07 (1975).

[17] M. Garcia-Munoz, G.M. Mason, J.A. Simpson, The isotopic composition of galactic cosmic-ray lithium, beryllium, and boron, Astrophys. J. Lett. 201 (L145) (1975).

[18] L. Jakubowski, M.J. Sadowski, J. Zebrowski, M. Rabinski, K. Malinowski, R. Mirowski, Ph. Lotte, J. Gunn, J.-Y. Pascal, G. Colledani, V. Basiuk, M. Goniche, M. Lipa, Cherenkov-type diamond detectors for measurements of fast electrons in the TORE-SUPRA tokamak, Rev. Sci. Instrum. 81 (2010) 013504.

[19] Y. Takabayashia, E.I. Fiks, Yu. L. Pivovarov, First studies of 500-nm Cherenkov radiation from 255-MeV electrons in a diamond crystal, Phys. Lett. A 379 (2015) 1032–1035.

[20] William R. Webber, private communications.

[21] C. Lopate, private communications.

[22] J.E. Ralph, Scintillation characteristics of diamond under alpha particle bombardment, Proc. Phys. Soc. 73 (1959) 233–238.

[23] Tom L. Nam, Hendrik J. Van Rijn, Rex J. Keddy, Paul J. Fallon, Joanne F. Schlimmer nee Andrews, US Patent 5, 128, 546, 1992.

[24] C. Bauer, I. Baumann, C. Colledani, J. Conway, P. Delpierre, F. Djama, W. Dulinski, A. Fallou, K.K. Gan, R.S. Gilmore, E. Grigoriev, G. Hallewell, S. Han, T. Hessing, K. Honschied, J. Hrubec, D. Husson, H. Kagan, D. Kania, R. Kass, W. Kinnison, K.T. Kniipfle, M. Krammer, T.J. Llewellyn, P.F. Manfredi, L.S. Pan, H. Pernegger, M. Pemicka, R. Piano, y Re, S. Roe, A. Rudge, M. Schaeffer, S. Schnetzer, S. Somalwar, V. Speziali, R. Stone, R.J. Tapper, R. Tesarek, W. Trischuk, R. Turchetta, G.B. Thomson, R. Wagner, P. Weilhammer, C. White, H. Ziock, M. Zoeller, Radiation hardness studies of CVD diamond detectors, Nucl. Instrum. Methods Phys. Res. A 367 (1995) 207–211.

[25] Charles E. Ashbaugh III, Radioactive and radiation treated gemstones, Radioact. Radiochem. 2 (1991) 42–57.

[26] J.J. Connell, C. Lopate, R.B. McKibben, A. Enman, Accelerator test of an angle detecting inclined sensor (ADIS) prototype with beams of ^{48}Ca and fragments, Nucl. Instrum. Methods Phys. Res. A 570 (2007) 399–413.

[27] M. Bouffard, J.J. Englemann, L. Koch, A. Soutoul, N. Lund, B. Peters, I.L. Rasmussen, The HEAO-3 cosmic ray isotope spectrometer, Astrophy. Space Res. 84 (1) (1982) 3–33.